

The GLUEX Start Counter Detector

E. Pooser^{a,b}, F. Barbosa^a, W. Boeglin^{b,*}, C. Hutton^a, M. Ito^a, M. Kamel^b, A. LLodra^b, N. Sandoval^a, S. Taylor^a, C. Yero^b, B. Zihlmann^a

^a*Thomas Jefferson National Accelerator Facility, Newport News, VA 23606, USA*

^b*Florida International University, Miami, FL, 33199, USA*

Abstract

The design, fabrication, calibration, and performance of the GLUEX Start Counter detector is described. The GLUEX experiment, staged in Hall D at the Thomas Jefferson National Accelerator Facility (TJNAF), primarily aims to study the rich spectrum of photo-produced mesons with unprecedented statistics. The coherent bremsstrahlung technique is implemented to produce a linearly polarized photon beam incident on a liquid H₂ target. A Start Counter detector was fabricated to properly identify the accelerator electron beam buckets and to provide accurate timing information. The Start Counter detector was designed to operate at photon intensities of up to $10^8 \gamma/s$ in the coherent peak and provides a timing resolution of ≈ 250 ps thus providing successful identification of the electron beam buckets to more than 99% accuracy. Furthermore, the Start Counter detector provides excellent solid angle coverage, $\sim 90\%$ of 4π hermeticity, a high degree of segmentation for background rejection, and is utilized in the level 1 trigger for the experiment. It consists of a cylindrical array of 30 thin scintillators with pointed ends that bend towards the beam at the downstream end. Magnetic field insensitive silicon photomultiplier detectors were selected as the readout system.

Keywords: GLUEX, Flash 250 MHz ADC, F1 TDC, Plastic Scintillator, Silicon Photomultiplier, Multi-Pixel Photon Counter, Time of Flight, Trigger, Particle Identification, Polishing Scintillators

1. Design

1.1. Overview

In this section we discuss the details of the GLUEX Start Counter design. The general engineering specifics pertaining to the scintillators, support structure, detector readout system and electronics are discussed.

The Start Counter (ST) detector, seen in Fig. 1, surrounds a 30 cm long super cooled liquid H₂ target while providing $\sim 90\%$ of 4π solid angle coverage relative to the target center. The primary purpose of the ST detector is, in coincidence with the tagger, to properly identify the electron beam bucket associated with detected particles produced via linearly polarized photons incident on the target. It is designed to operate at tagged photon intensities of up to $10^8 \gamma/s$ in the coherent peak.

*Corresponding Author

Email address: boeglinw@fiu.edu (W. Boeglin)

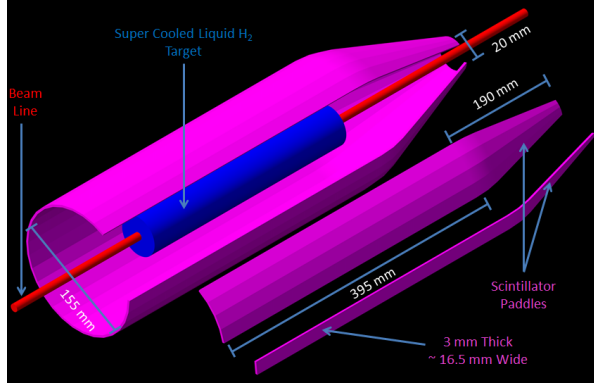


Figure 1: Start Counter geometry.

Moreover, the ST has a high degree of segmentation for background rejection, is utilized in particle identification, and is a primary component of the level 1 trigger of the GLUEX experiment during high luminosity running[1].

The ST detector consists of an array of 30 scintillators with pointed ends that bend towards the beam at the downstream end. EJ-200 scintillator material from Eljen Technology[2], which provides a decay time of 2.1 ns and a long attenuation length[3], was selected for this application. The amount of support structure material was kept to an absolute minimum in the active region of the detector and is made up of low density Rohacell[4]. Silicon Photomultiplier (SiPM) detectors were selected as the readout system. The detectors are not affected by the high magnetic field produced by the superconducting solenoid magnet. Moreover, the SiPMs were placed as close as possible to the upstream end of each scintillator element, thereby minimizing the loss of scintillation light[1].

1.2. Scintillator Paddles

Each individual paddle of the Start Counter was machined from a long, thin, polyvinyltoluene plastic EJ-200 scintillator bar that was diamond milled to be 600 mm in length, 3 mm thick, and 20 ± 2 mm wide, by Eljen Technology. Each scintillator was bent around a highly polished aluminum drum by applying localized infrared heating to the bend region. The bent scintillator bars were then sent to McNeal Enterprises Inc.[5], a plastic fabrication company, where they were machined to the desired geometry illustrated in Fig. 2.

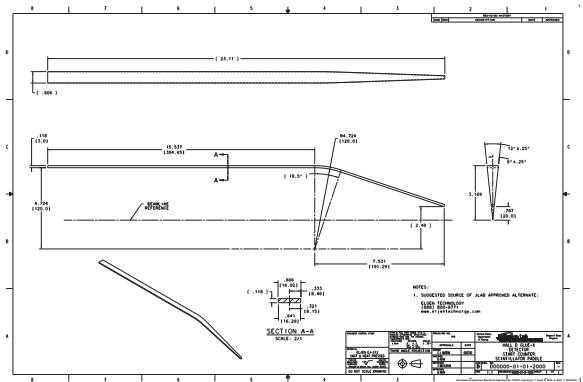


Figure 2: Start Counter single paddle geometry.

The paddles consist of three sections and are described from the upstream to the downstream end of the target. The straight section is 39.465 cm in length while being oriented parallel to both the target cell and beamline.. The bend region is a 18.5° arc of radius 120 cm and is downstream of the straight section. The tapered nose region is downstream of the target chamber and bends towards the beam line such that the tip of the nose is at a height of 2 cm above the beam line.

After the straight scintillator bar was bent to the desired geometry, the two flat surfaces that are ori-

ented orthogonal to the wide, top and bottom, surfaces were cut at a 6° angle. During this process,
⁶⁵ the width of the top and bottom surfaces were machined to be 16.92 mm and 16.29 mm wide respectively. Thus, each of the paddles may be rotated 12° with respect to the paddle that preceded it so
⁷⁰ that they form a cylindrical shape with a conical end. This geometrical design for the ST increases solid angle coverage while minimizing multiple scattering.

1.3. Support Structure

The ST scintillator paddles are placed atop a low
⁷⁵ density Rohacell ($\rho = 0.075 \text{ g/cm}^3$) foam support structure which envelopes the target vacuum chamber seen in Fig. 3. The Rohacell, which is 11 mm

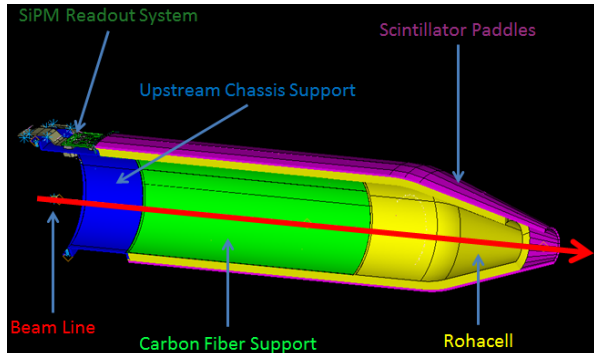


Figure 3: Cross section of the Start Counter detector.

thick, is rigidly attached to the upstream support chassis and extends down the length of paddles
⁸⁰ however, not to include the last few centimeters of the conical nose section. Glued to the inner diameter of the Rohacell support structure are 3 layers of carbon fiber ($\rho = 1.523 \text{ g/cm}^3$) each of which are 650 μm thick. A cross section of the ST can be
⁸⁵ seen in Fig. 3 where the carbon fiber is visible. The

carbon fiber provides additional support during the assembly process as well as long term rigidity.

1.4. SiPM Readout Detectors

The selected readout for each scintillator bar is
⁹⁰ the magnetic field insensitive Hamamatsu S10931-050P surface mounted Multi-Pixel Photon Counters (MPPCs)[6]. An individual $3 \times 3 \text{ mm}^2$ MPPC, also known as a SiPM, in the aforementioned configuration is comprised of 3600 individual, $50 \times 50 \mu\text{m}^2$,
⁹⁵ Avalanche Photo-Diode (APD) pixel counters operating in Geiger mode. The signal output from each SiPM is the total sum of the outputs from all 3600 APD pixels[7]. The scintillation light from an individual scintillator bar is collected by an array of four of these SiPMs.

The SiPM readout detectors are housed in a ceramic case which is surface mounted to a custom fabricated Printed Circuit Board (PCB). The PCB is held in a fixed position while being attached to the lip of the upstream chassis *via* two screws as illustrated in Fig. 4. The individual ST scintillators are coupled *via* an air gap ($< 250 \mu\text{m}$) to groups of four SiPMs set in a circular arrangement as can be seen in Fig. 4.



Figure 4: ST1 of Start Counter read out system. The ST1's are rigidly attached to the upstream support chassis. Approximately 72% of the scintillator light is collected at the upstream end.

110 1.5. Readout Electronics

The SiPMs reading out one individual paddle, are current summed prior to pre-amplification. The output of each preamp is then split; buffered for the Analog to Digital Converter (ADC) output, and amplified for the Time to Digital Converter (TDC) output by a factor five relative to the ADC. The ADC outputs are readout *via* JLab VME64x 250 MHz Flash ADC modules while the TDC outputs are input into JLab leading edge discriminators, followed by a high resolution 32 channel JLab VME64x F1TDC V2 module. Furthermore, each group of four SiPMs utilizes a thermocouple for temperature monitoring. There are 120 SiPMs in total, for a total of 30 pre-amplifier channels as seen Fig. 5.

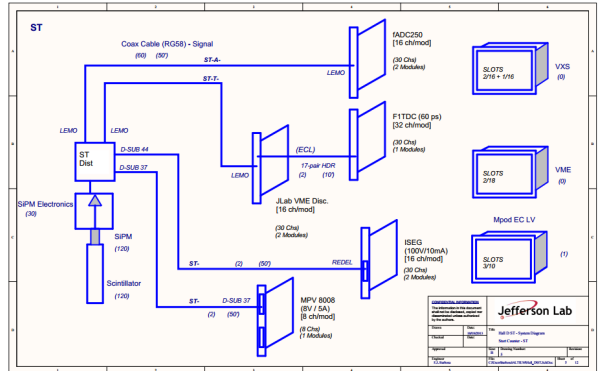


Figure 5: Start counter readout electronics diagram.

125 There are three components that comprise the ST detector readout system. The first component is the ST1 which holds 3 groups of 4 SiPMs as can be seen in Fig. 4. In order to mimic the geometry of the 30 paddle design one group of SiPM's is rotated by 12° relative to the central group, while 130 the other adjacent group is rotated by -12° . One ST1 unit will collect light from three paddles indi-

vidually. The ST1 implements the current sum and bias distribution per group of 4 SiPMs. It also has a thermocouple for temperature monitoring.

135 The second component is the ST2, seen in Fig. 6, is a Printed Circuit Board (PCB) that houses the signal processing electronics of the readout system. It has 3 channels of pre-amplifiers, 3 buffers, and

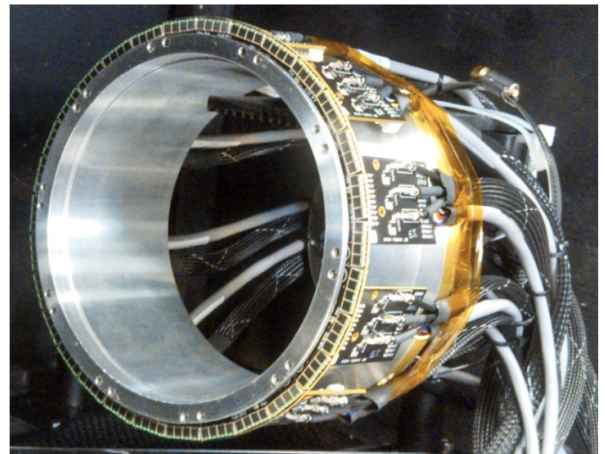


Figure 6: Fully assembled ST readout system.

140 3 factor five amplifiers. Furthermore, it has 3 bias distribution channels with individual temperature compensation *via* thermistors. The ST2 is attached to the ST1 *via* 90° hermaphroditic connector.

145 The third component of the readout system, the ST3 seen in Fig. 7, provides interface to the power and bias supplies. It also routes the ADC and TDC outputs as well as the thermocouple output. The ST3 connects to the ST2 *via* a signal cable assembly seen in Fig. 6 and Fig. 7. The ST3 is installed upstream of the Start Counter and next to the beam pipe.



Figure 7: Start counter ST3 readout system.

2. Fabrication

In order to successfully identify the 2 ns electron beam bunch structure delivered by the CEBAF to within 99% accuracy, the GLUEX Start Counter time resolution is required to be < 350 ps. In the following section the details of polishing and characterizing machined scintillators, as well as the construction of the Start Counter are discussed.

2.1. Polishing Machined Scintillators

The surfaces of the machined scintillators incurred a plethora of surface defects and chemical contaminants known to harm scintillator surfaces while undergoing edge polishing at McNeal Enterprises. Therefore, in an effort to recover the scintillator surfaces and performance capabilities, polishing was required.

Prior to polishing the machined scintillators, a coarse measurement of the paddles performance was conducted to understand the magnitude of damage the paddles had incurred, relative to prototypes, as a result of mishandling. The time resolution and light output was measured at three precise locations along the length of the scintillators. One measurement was taken in the middle of the

straight section, one in the middle of the bend, and one at the tip of the nose.

Figure 8 illustrates the erratic fluctuation and poor performance that existed from paddle to paddle prior to polishing. On average the 50 paddles

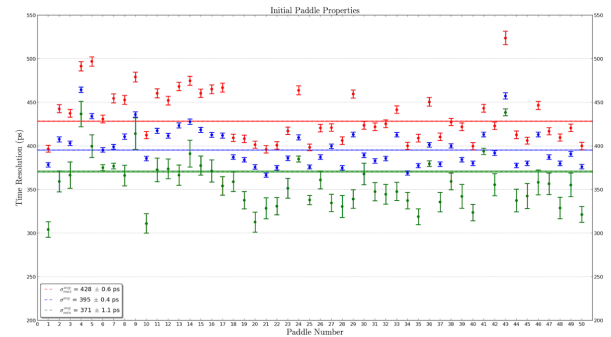


Figure 8: Coarse time resolution measurements prior to polishing. Paddle number is on the x-axis and time resolution in ns is on the y-axis. The red points are the resolutions in the bend region, the blue points are the weighted average of the three measurements, and the green points are the resolutions at the tip of the nose. The horizontal lines are the weighted averages of the individual measurements.

did not meet the design resolution of 350 ps.

To polish the machined scintillator surfaces, Buehler Micropolish II deagglomerated 0.3 μm alumina suspension was utilized[8]. The polishing suspension was diluted with a 5:1 ratio of de-ionized H₂O to alumina and applied to a cold, wet 6" \times 0.5" Caswell Canton flannel buffering wheel[9] operated at < 1500 RPMs. All surfaces of the scintillators were carefully buffed until all large, uniform surface defects were removed. In order to eliminate small, localized surface defects hand polishing with a soft NOVUS premium Polish Mate microfilament cloth[10] and diluted polishing suspension was applied. These polishing procedures made the scintillators void of virtually all scratches and surface

defects.

Once the appropriate polishing procedures had been developed and implemented the surface quality was greatly improved as can be seen in Fig. ?? which illustrates the same scintillator paddle before and after polishing. A red laser beam was shone

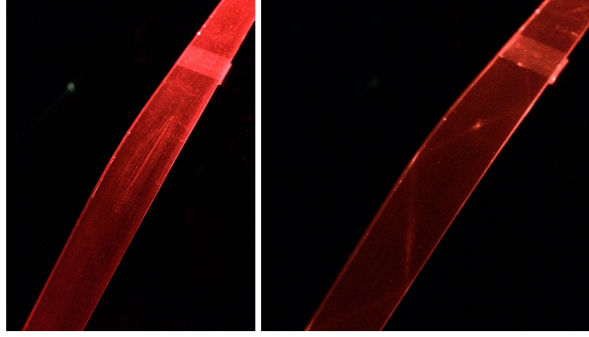


Figure 9: Effects of polishing scintillators. Left: non-diffuse laser incident on an edge, before polishing, at the upstream end of the straight section. Right: non-diffuse laser incident on the same edge, after polishing, at the upstream end of the straight section.

into the scintillator medium from the upstream end aimed at one edge so that the total internal reflection towards the tip of the nose was visible. The unpolished scintillator had such poor surface quality that the reflections in the bend region could not be seen due to the multiple scattering of light at the scintillator boundaries. However, the reflections in the polished scintillator can clearly be seen traversing down through the nose region.

Once the scintillators were polished, their performance was remeasured so that a quantitative measure of the polishing effects were understood. The measurements were performed in an identical manner outlined above and the pre-polished results were illustrated in Fig. 8. As expected, the time resolutions were greatly improved as seen in Fig. ??.

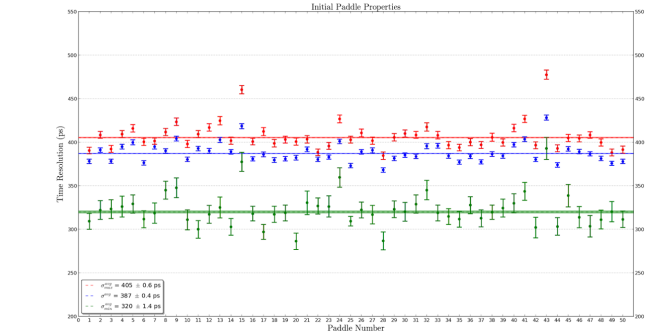


Figure 10: Coarse time resolution measurements after polishing. The details are identical to Fig. 8

average, at the tip of the nose, the scintillators exhibited a $\approx 15\%$ improvement in time resolution. Moreover, there was a substantial reduction in erratic fluctuations in performance.

2.2. Testing Machined Scintillator Paddles

Each of the 50 machined scintillators were tested to study light output and time resolution. They were measured in an identical manner utilizing a custom fabricated test stand shown in Fig. ???. The test stand allows each scintillator paddle to be measured in an identical and reproducible fashion. There exist 12 precise locations in which a ^{90}Sr source and trigger PMT can be placed so that each of the 50 scintillators are tested at the same locations. More specifically 4 locations in the straight section, 3 in the bend, and 5 in the nose were tested.

References

- [1] E. Pooser, The GlueX start counter and beam asymmetry Σ in single π^0 photoproduction, Ph.D. thesis, Florida International University (2016).
- [2] <http://www.eljentechnology.com/>.
- [3] General Purpose Plastic Scintillator EJ-200, EJ-204, EJ-208, EJ-212, technical note available at

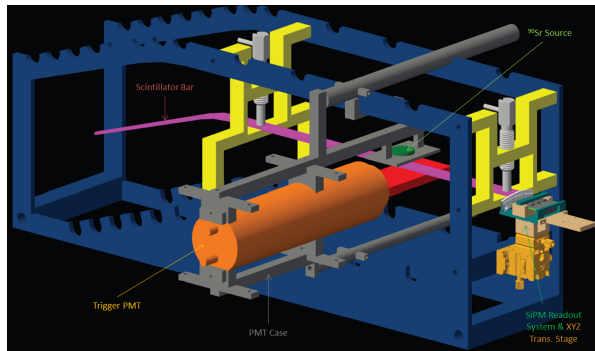


Figure 11: CAD Drawing of custom test stand. The test stand was used in the misalignment studies.

[http://www.eljentechnology.com/images/products/
data_sheets/EJ-200_EJ-204_EJ-208_EJ-212.pdf](http://www.eljentechnology.com/images/products/data_sheets/EJ-200_EJ-204_EJ-208_EJ-212.pdf).

- 245 [4] <http://www.rohacell.com>.
- [5] <http://www.mcnealplasticmachining.com/>.
- [6] <http://www.hamamatsu.com/us/en/index.html>.
- [7] Multi-Pixel Photon Counter, technical note available at https://halldweb1.jlab.org/wiki/images/4/49/S10362-33_series_kapd1023e05.pdf.
- 250 [8] [https://shop.buehler.com/consumables/
grinding-polishing/polishing-suspensions/
alumina-suspensions](https://shop.buehler.com/consumables/grinding-polishing/polishing-suspensions/alumina-suspensions).
- [9] [http://www.caswellplating.com/
buffing-polishing/buffing-wheels/
canton-flannel-wheels.html#](http://www.caswellplating.com/buffing-polishing/buffing-wheels/canton-flannel-wheels.html#).
- 255 [10] https://www.novuspolish.com/polish_mates.html.